Supporting Information

High-Electric-Field-Induced Hierarchical Structure Change of Poly(vinylidene Fluoride) as Studied by the Simultaneous Time-resolved WAXD/SAXS/FTIR Measurements and the Computer Simulations

Kohji Tashiro,[1*] Hiroko Yamamoto,[2] Sreenivas Kummara,[1] Tomohiko Takahama,[1]
Kouki Aoyama,[3] Hiroshi Sekiguchi,[3] and Hiroyuki Iwamoto[3]

[1] Department of Future Industry-oriented Basic Science and Materials, Graduate School of Engineering, Toyota Technological Institute, Tempaku, Nagoya 468-8511, Japan

[2] Aichi Synchrotron Radiation Center, Aichi Science and Technology Foundation, 250-3 Minami-yamaguchi, Seto 489-0965, Japan

[3] Japan Synchrotron Radiation Research Institute, SPring 8, Kouto 1-1-1, Sayo 679-5198, Japan

<Supporting Information 1> WAXD and SAXS patterns measured for the original PVDF30 and 10 films

(1) PVDF30 Film

Figure S1-1 shows the 2D WAXD and SAXS patterns of the original PVDF30 sample measured in the *edge*, *through* and *end* directions. Mostly the crystalline α form occupies the sample and the smaller amount of the β form is detected additionally. The degree of crystallite orientation in the sheet plane is low as known from the nearly homogeneous ring patterns detected in the *through* pattern, but the careful investigation revealed the slightly heterogeneous intensity distribution along

the rings. For example, the 020 peak of the α form, which is now expressed as 020(α) for simplicity, shows the relatively stronger intensity in the direction ±45° from the vertical axis (or the machine direction, MD). The 002(α) diffraction also has a relatively stronger intensity in ±45° direction. Therefore, the *b*(α) and *c*(α) axes are oriented in the diagonal direction of the sheet plane, although the orientation is not very high. The *edge* and *end* patterns are similar to each other. The 2D WAXD pattern along the *edge* direction is apparently of the highly-oriented sample, but it comes from the preferential in-plane orientation of the *b*(α) and *c*(α) axes. The 100(α) peak is detected mostly in the *edge* (and *end*) pattern, not in the *through* pattern, indicating that the *a*(α) axis is preferentially oriented along the normal to the film sheet. The rough illustration of the orientation of the α-form unit cell axes is shown in Figure S1-1 (d).

The orientation of the crystal form β is also estimated from the characteristic diffraction patterns. The 020(β) diffraction peak is stronger in the *end* and *edge* patterns. The 001(β) peak is detected relatively strongly along the equatorial line, indicating that the *c*(β) axis directs rather near the equatorial direction. The *b*(β) axis is oriented in the direction normal to the film sheet.

The SAXS *through* pattern shows the long period peaks in the direction parallel to the *c*(α) axis. The SAXS peak of the β form is difficult to detect because of the relatively small content. If we assume that the lamellar normal and the chain axis are parallel to each other, the lamellar stacking mode can be drawn as illustrated in Figure S1-1 (d). The streaks observed along the equatorial line in the edge and end patterns are originated from the X-ray scattering from the thin sample edge.

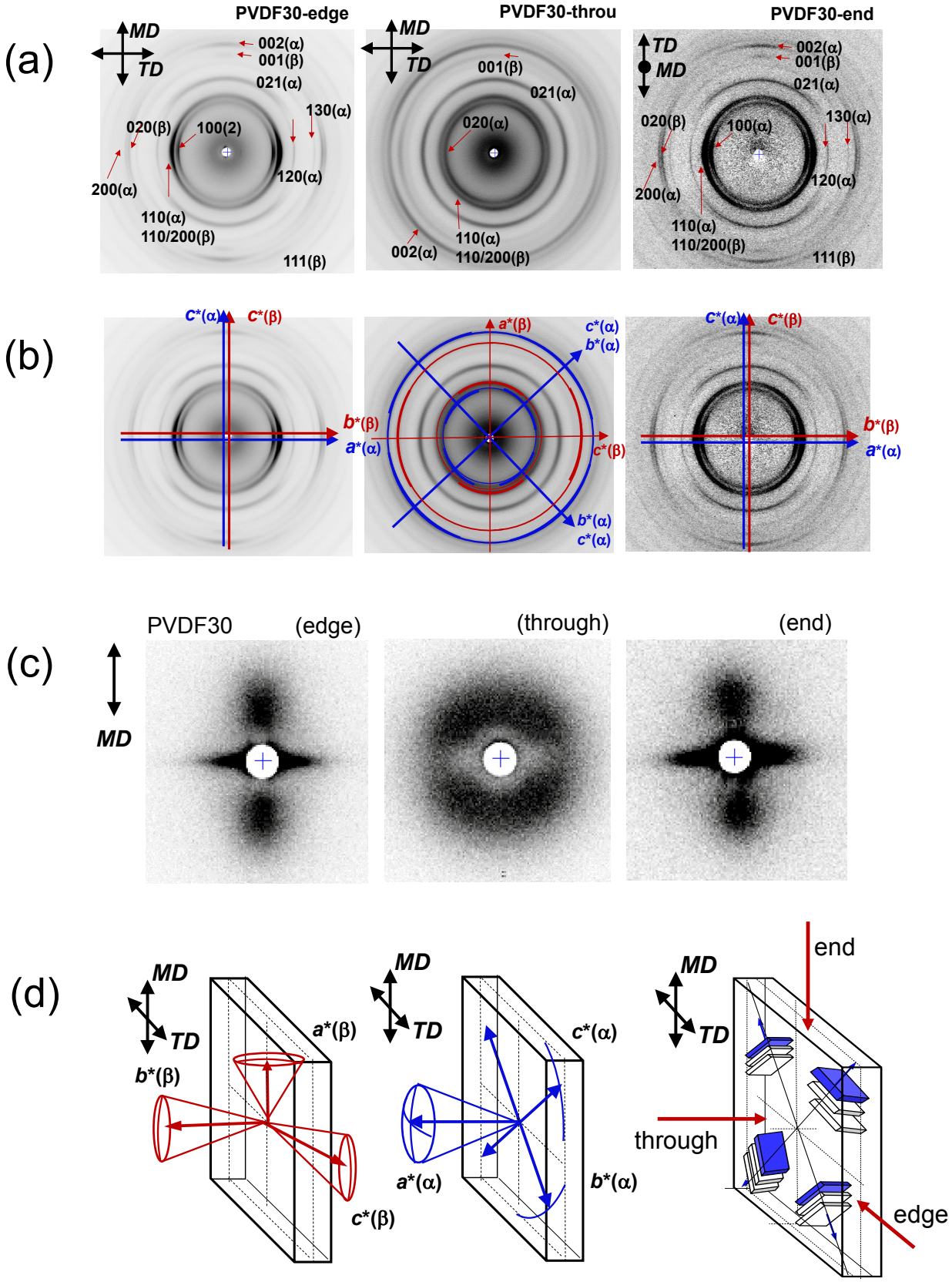

Figure S1-1 (a) (b) 2D WAXD and (c) SAXS patterns of PVDF30 film measured by irradiating the X-ray beam (red arrow) along the *edge*, *through* and *end* directions. The orientations of the unit cell axes and the stacked lamellar structure are illustrated in (d).

(2) PVDF10 Film

Figure S1-2 shows the 2D WAXD and SAXS patterns measured for the PVDF10 film in the 3 directions. The diffraction peaks of the β form are relatively strong. The 020(β) peak is observed clearly in the *edge* and *end* WAXD patterns. The 001(β) peak is strong in the transverse direction (TD) and the 200/110(β) peak is relatively strong in the MD. The spatial orientation of the unit cell axes is illustrated in Figure S1-2 (d). The orientation of the α-form crystallites is not very high. The *b*(β) and *a*(α) axes are oriented mainly in the direction normal to the sheet plane. It must be noted that the chain axis of the β form orients mainly along the TD, not the MD. The observed long period peak in the SAXS patterns is interpreted as the stacked lamellar structure illustrated in Figure S1-2 (d). If the chain axis is assumed to be parallel to the lamellar normal, the lamellae of the β form are stacked along the TD, while those of the α form along the MD, as illustrated there. The lamellae shown in red color might correspond to those of the β form since the *c* axis is preferentially oriented to the TD. The lamellae of the α form (blue color) are in an approximation along the MD because the *c* axis is in this direction. The streaks observed along the equatorial line in the edge and end patterns are originated from the parasitic X-ray scattering coming from the thin sample edge.

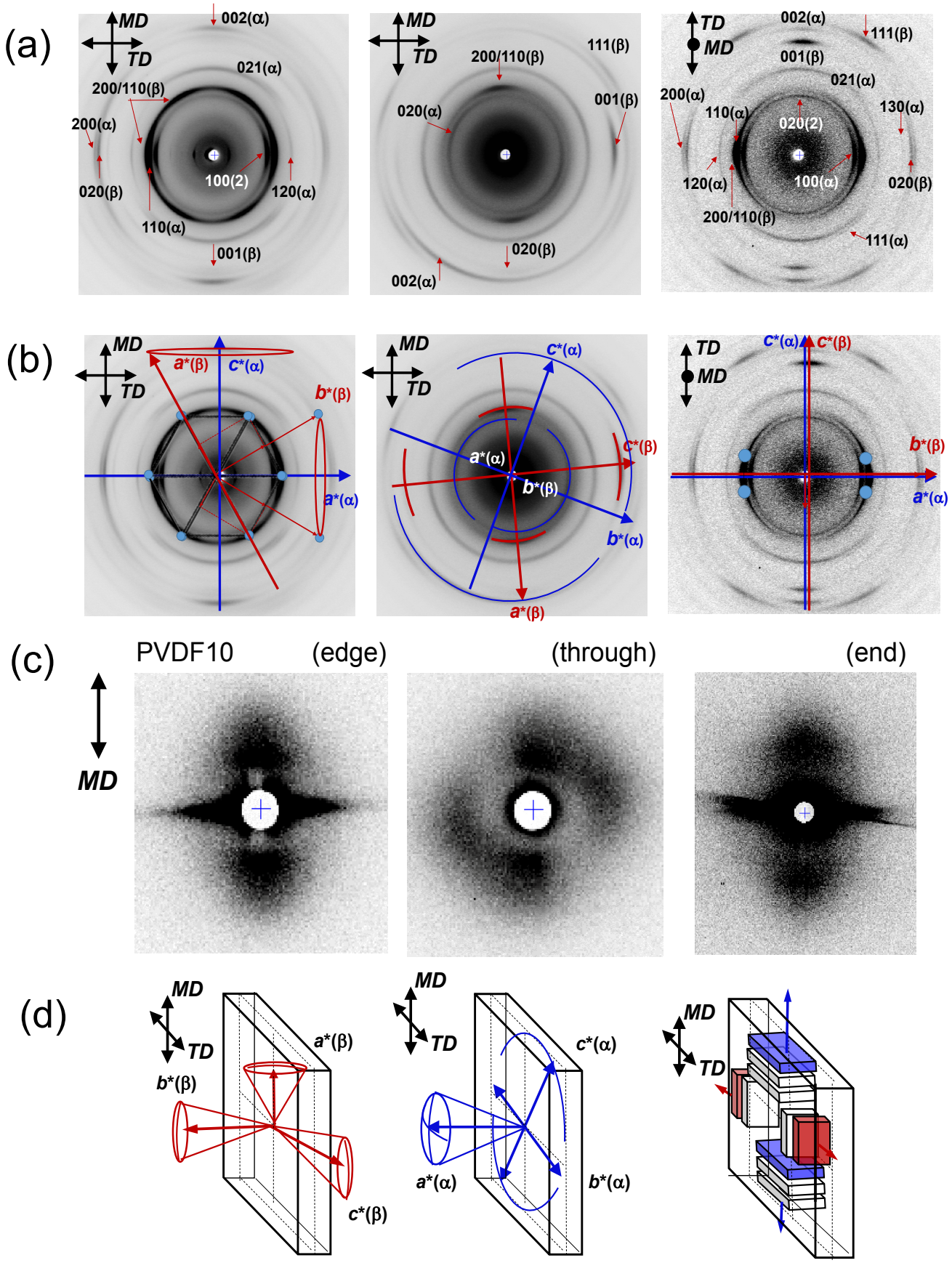

Figure S1-2 (a) (b) 2D WAXD and (c) SAXS patterns of PVDF10 film measured by irradiating the X-ray beam (red arrow) along the *edge*, *through* and *end* directions. The orientations of the unit cell axes and the stacked lamellar structure are illustrated in (d).

<Supporting Information 2> Snapshots of the System for the High-Voltage Experiments

Some of the important experimental parts in the present study are shown using the following snapshots (Figure S2-1).

(a) A plastic holder with aluminum electrodes on the sample surfaces.

(b) The aluminum electrode evaporated on the sample surface and a thin aluminum tape as the electric wire pasted on the electrode using a silver paste.

(c) The miniature FTIR spectrometer set at the center of the sample position. The WAXD detector of a blue color frame is seen in the right side.

(d) The SAXS detector set at about 3 m downstream position from the sample *via* a vacuum pipe.

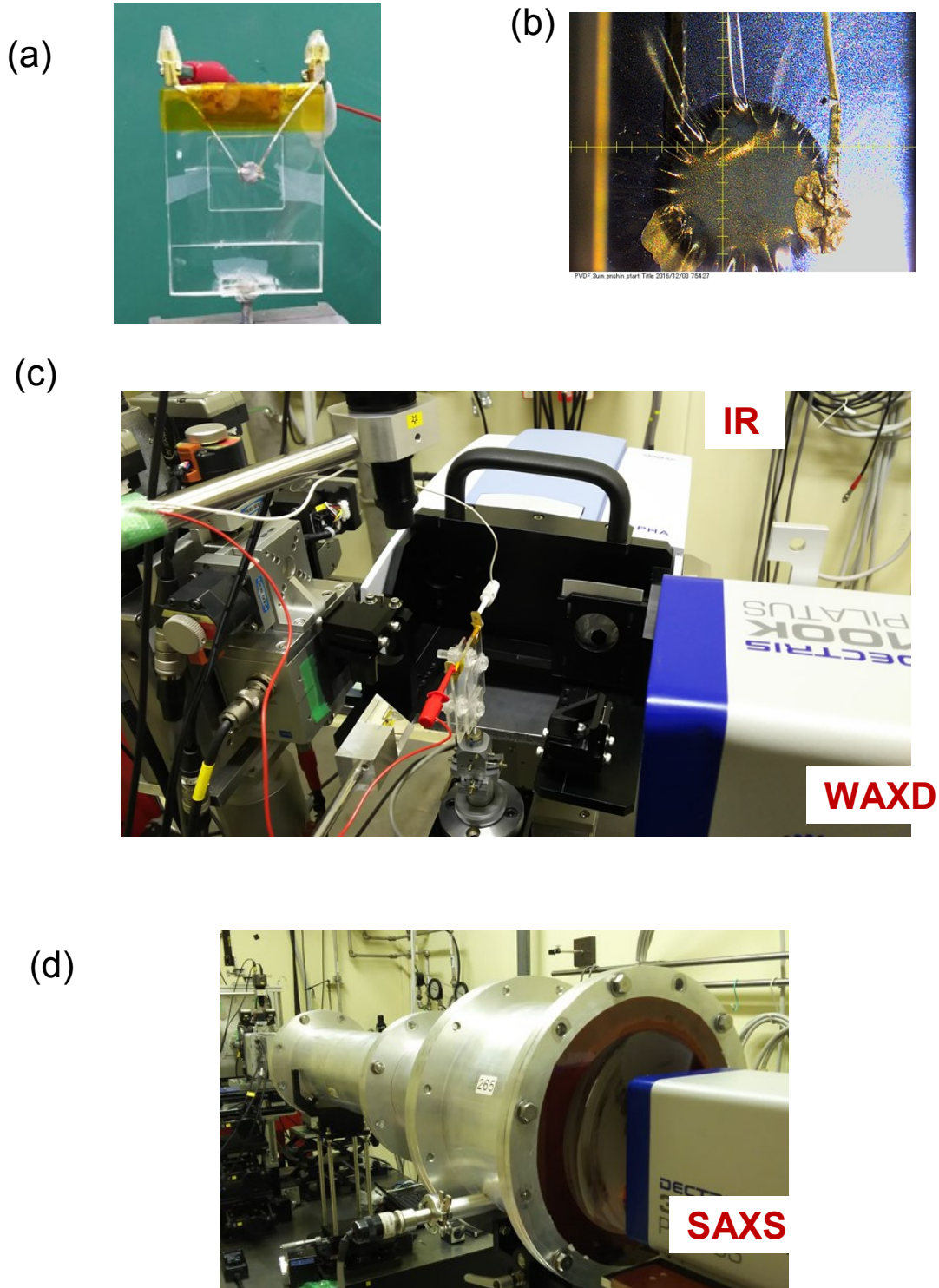

Figure S2-1. Pictures of (a) a plastic holder of a film with Al electrodes evaporated on the both sides, (b) the electrode parts connected to the thin Al cables using a silver paste, (c) the FTIR spectrometer and WAXD detector installed surrounding the sample holder, and (d) the SAXS detector set about 3 m distant from the sample position *via* a vacuum pipe.

<Supporting Information 3>

(1) X-ray Diffraction Profiles and Miller Indices of PVDF β, α and δ Forms

The 1D X-ray diffraction profiles and the Miller indices of the peaks are shown in Figure S3-1. For reference, the crystallographic data are shown below.

(1) β form $a = 8.58$ Å, $b = 4.91$ Å, c (chain axis) = 2.56 Å (Orthorhombic, Space group $Cm2m$)

(2) α form $a = 4.96$ Å, $b = 6.94$ Å, $c = 4.62$ Å, $\beta = 90^{o}$ (Monoclinic, Space group $P2_1/c$)

(3) δ form $a = 4.96$ Å, $b = 6.94$ Å, $c = 4.62$ Å (Orthorhombic, Space group $P2_1cn$)

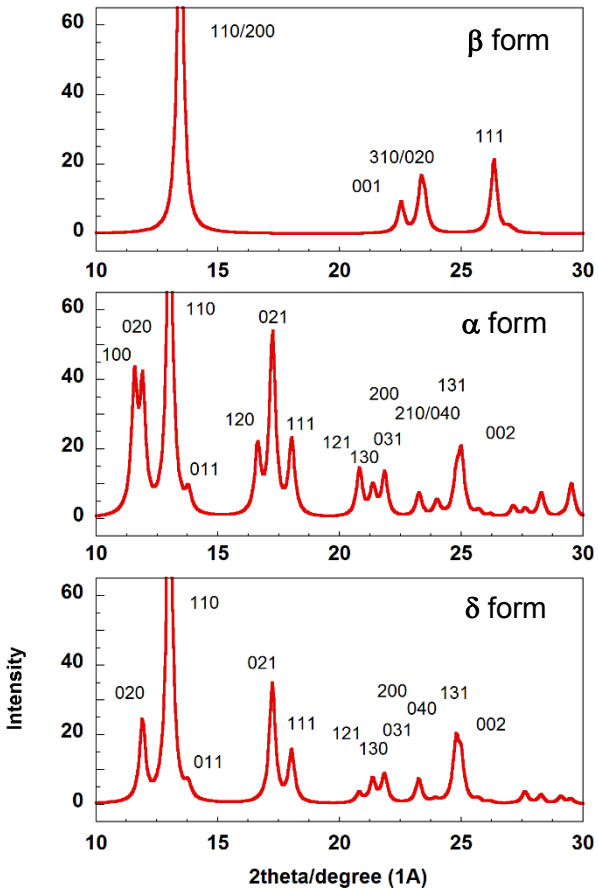

Figure S3-1 X-ray diffraction profiles and Miller indices of the unoriented PVDF β, α and δ forms, where the wavelength of the incident X-ray is 1.0 Å.

Reference K. Tashiro, Crystal Structure and Phase Transition of PVDF and Related Copolymers, Ferroelectric Polymers: Chemistry, Physics, and Technology (H. S. Nalwa edt.), Marcel Dekker Inc., p.63 - 182 (**1995**).

(2) X-ray diffraction profiles of PVDF30 film before and after the corona-poling

The X-ray diffraction patterns and the diffraction profiles were collected for the PVDF30 films before and after the corona-poling treatment at room temperature. The corona poling is a method to supply a high electric field to the film. As illustrated in Figure S3-2, the sample is put on a metal plate connected to a grounding wire. A sharp needle is set at the position about 2 cm above the metal plate. The high voltage of about 5 – 8 kV is applied to a needle, from which the shower of corona is emitted and covers the sample. The film is strongly pressed to the metal plate during the corona charging.

Figure S3-3 shows the X-ray diffraction patterns measured from the *through* and *edge* directions of the PVDF30 film before and after the corona charging treatment. The 1D diffraction profiles obtained along the equatorial and meridional lines are also shown there with the Miller indices of the various diffraction peaks.

The PVDF α form shows the 100 peak, which disappears in the δ form obtained by the poling treatment of the α form. Similarly the several peaks (120, 130 etc.) also disappear. In the original film the 100 peak is not detected in the *through* pattern but it is detected relatively strongly in the *edge* direction. This indicates that the *a* axis of the α form orients toward the normal to the film surface. After the poling treatment, the α form transforms to the δ form, the *a* axis of which is the polar axis and is oriented to the film normal. Therefore, the whole pattern does not change very much apparently before and after the poling. But the symmetry is different between these two phases, and the several typical diffraction peaks are not detected in the film after the poling treatment, as mentioned above.

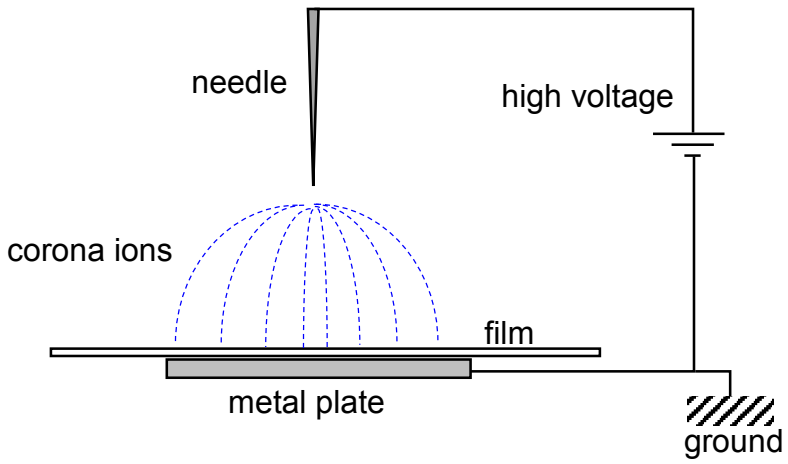

Figure S3-2 Simple device for the corona poling treatment of a film.

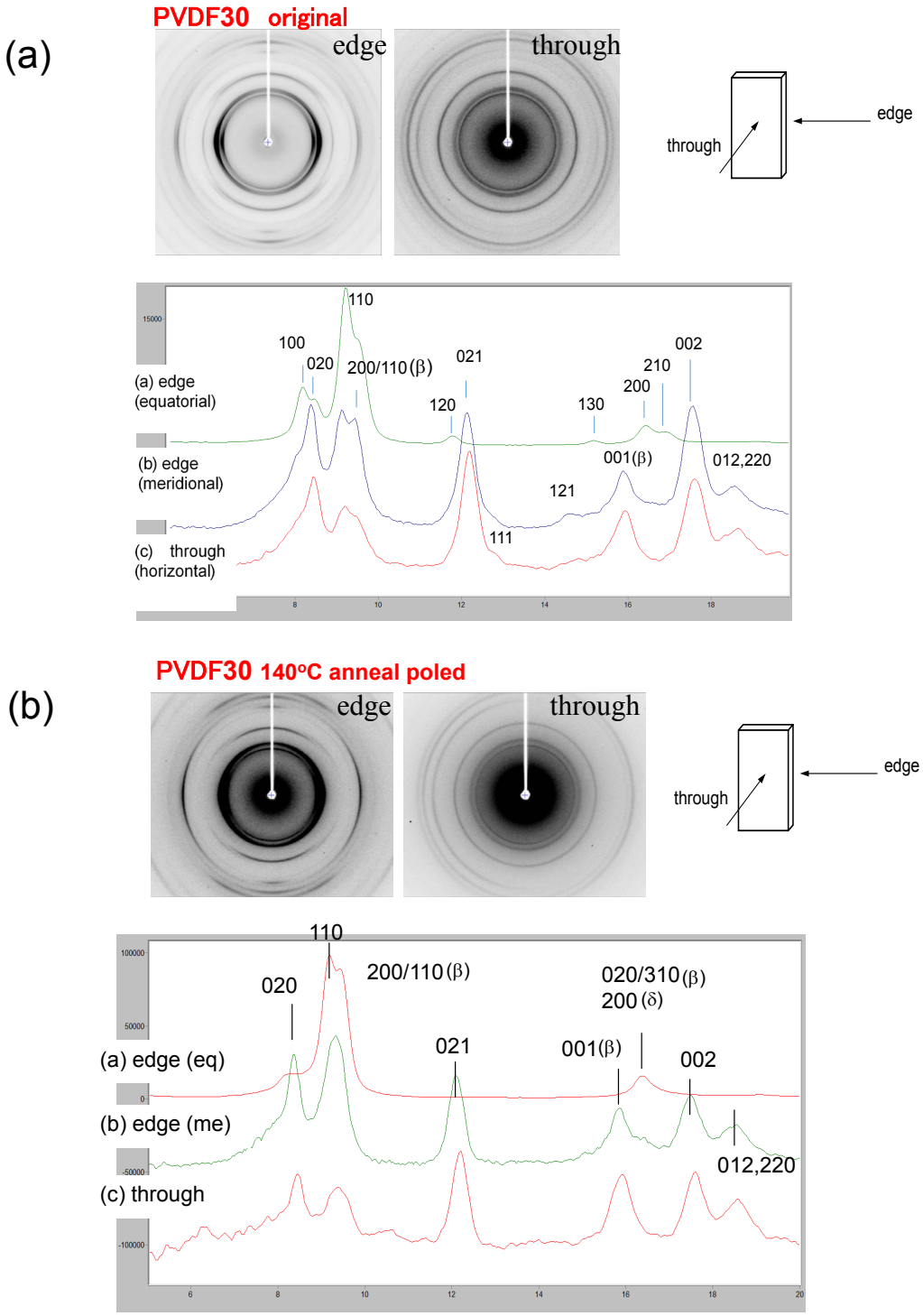

Figure S3-3 X-ray diffraction profiles measured in the various directions of the PVDF30 film (a) before and (b) after the corona poling. The wavelength of an incident X-ray is 1.0 Å. The 1D diffraction profiles were obtained by integrating the 2D patterns along the equatorial (eq) or meridional (me) line in a certain width.

<Supporting Information 4> WAXD and SAXS data collected for PVDF10 film with the synchrotron X-ray beam irradiated on the fixed sample position

As mentioned in the text, the experiment with the incident X-ray beam position fixed at a particular point of the electrode caused the dielectric breakdown quite easily. This tendency was stronger for PVDF30 film than PVDF10 film, since the V_{max} was 9 - 10 kV in the former case and 3 - 5 kV in the latter case for giving the similar electric field strength of about 300 MV/m. The WAXD, SAXS and IR spectral data measured successfully for the PVDF10 film are described here.

In the actual experiment, the X-ray beam was incident in the *through* direction (perpendicularly to the electrodes) at a particular *fixed position* of the film. A series of snapshots of the observed WAXD and SAXS patterns are shown in Figure S4-1.

<WAXD> The 100 diffraction peak of the α form, which is expressed as 100(α) afterward, should have disappeared in the early stage of the first cycle because of the transformation from the α form to the δ form, but originally the 100(α) peak itself was low in intensity in the *through* direction [see the supporting information 1], and the clear intensity change of the 100(α) peak could not be detected in this measurement. On the other hand, the 001(β) and 111(β) peaks of the β form were detected comparatively clearly. In the first cycle (#1 and #2 in Figure S4-1), the 020(β) and 001(β) peaks of the β form increased the intensity gradually with an increase of the electric field strength (up to + 300 MV/m). In the second cycle from +300 ~ 0 MV/m (#3), the peak intensity did not change very much. In the range from 0 ~ -300 MV/m (#3 - #5), the 001(β) intensity became stronger and showed the

maximum at around -200 MV/m, while the 111(β) intensity became weaker there. When this type of measurement was repeated, the X-ray diffraction peak became gradually weaker because of the sample damage, making the quantitative intensity evaluation hard. Only qualitatively, the 001(β) intensity repeated the change following the inversion of the electric field, and the 111(β) diffraction peak behaved oppositely. Figure S4-2 shows the electric field strength dependence of the integrated intensity of the 001(β) peak where only the 1st cycle data are presented since the data in the second cycle were quite noisy. The intensity increased at around 200 MV/m region although the S/N ratio was not very high. The additional peak at around 0 MV/m is ambiguous, which was confirmed by the sample-position-scanning experiment described in the text.

<SAXS> As shown in Figure S4-1 (b), the SAXS pattern itself did not change very much, though the total intensity faded gradually with the increase of the X-ray exposure time. The 1D profiles were obtained along the MD and TD, as shown in Figure S4-3 (a), where the Iq^2 is plotted against q [I: intensity and q: scattering vector, $q = (4\pi/\lambda)\sin(\theta)$, by taking the Lorentz correction for the lamellar structure into account]. The peak position was shifted toward the lower q side slightly, indicating the quite small increase of the long period of the stacked lamellae. The integration of Iq^2-q curve was performed in the observed q range, a measure of the invariant Q_o. As shown in Figure S4-3, a large increase of the integrated value was observed in the negative high E region starting at around ‐200 MV/m, where the 001(β) WAXD intensity became maximal. The SAXS intensity (more exactly, Q_o value) originated from the stacked lamellar structure is approximately proportional to the density difference (Δρ) between the crystalline and amorphous phases as well as the crystallinity (X_c). It is

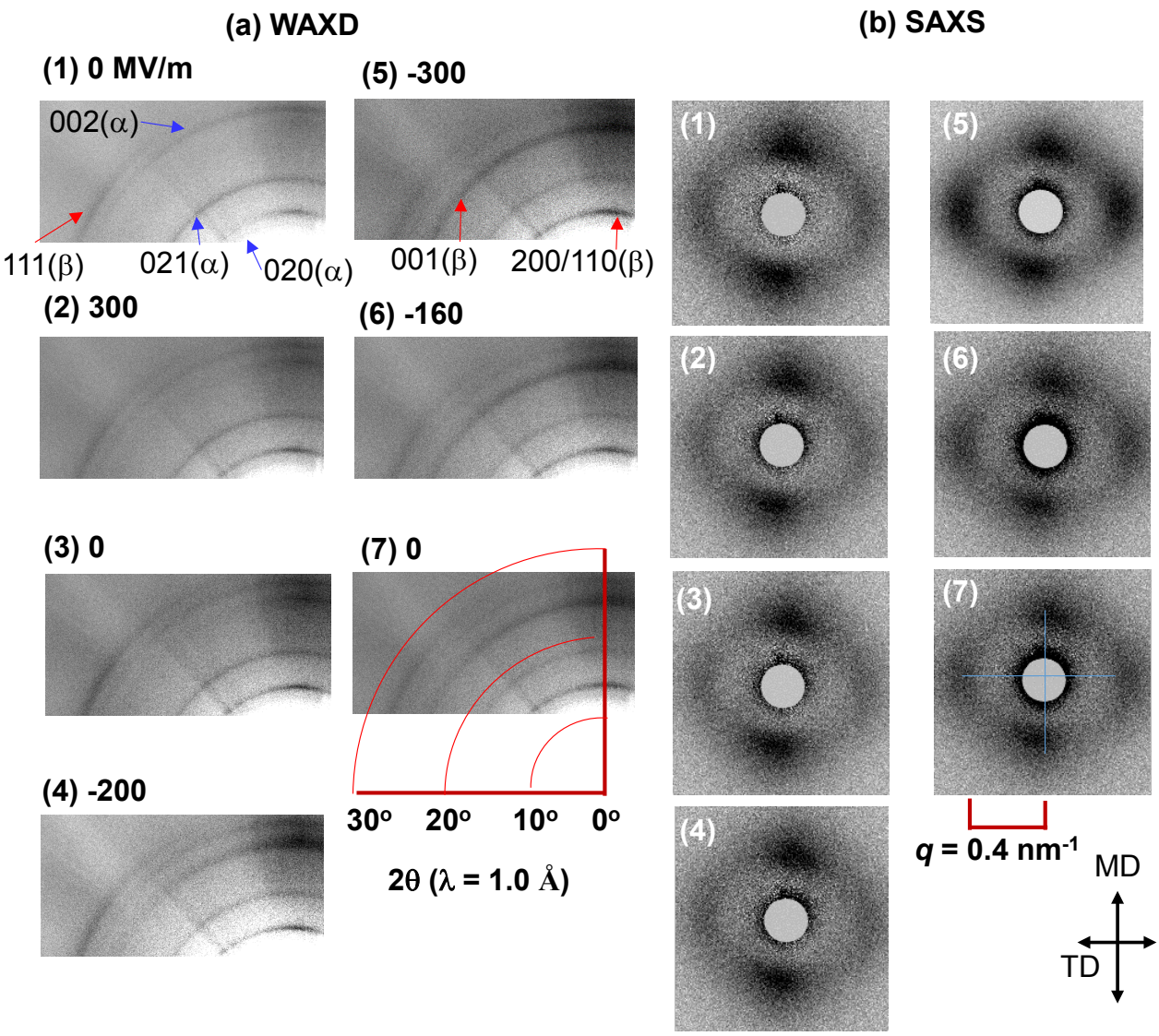

Figure S4-1. (a) 2D WAXD patterns and (b) 2D SAXS patterns measured for the PVDF10 film in the *through* direction under the application of the cyclic electric field. The MD is along the vertical direction. The indexing of the detected peaks is referred to in the supplementary information 1. The 001(β) peak intensity of the β form became maximal at -300 MV/m, where the SAXS peak along the TD direction, assigned tentatively to the stacked lamellar structure of the β form, increased the intensity correspondingly. The scales are given in the 2θ unit for the WAXD (λ = 1.0 Å) and in the q unit for the SAXS data, where $q = (4\pi/\lambda)\sin(\theta)$.

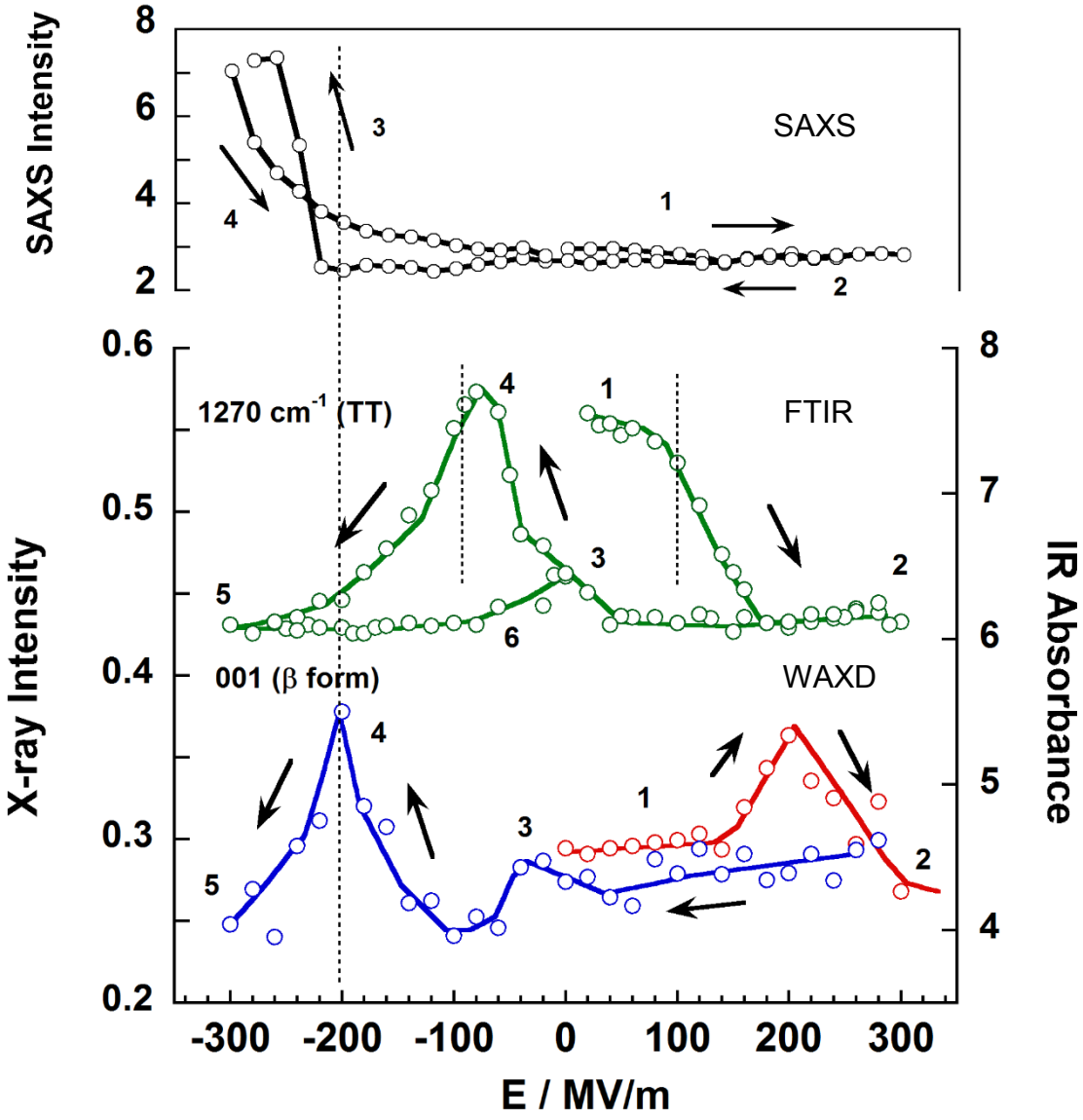

Figure S4-2 Electric field strength dependence of the SAXS integrated intensity (TD component in Figure S1-2), the IR absorbance [$\nu_s(CF_2)$ of the trans-zigzag form, 1275 cm^{-1}] and the WAXD 001(β) diffraction intensity evaluated for the PVDF10 film subjected to an electric field at the fixed position. The SAXS data and the IR data are quoted from Figures S4-3 and S4-4, respectively. The data in the first cycle are plotted since the diffraction intensity decreased remarkably in the second cycle. The colors of the curves are only for the clear distinguish of the routes (indicated by the numbers).

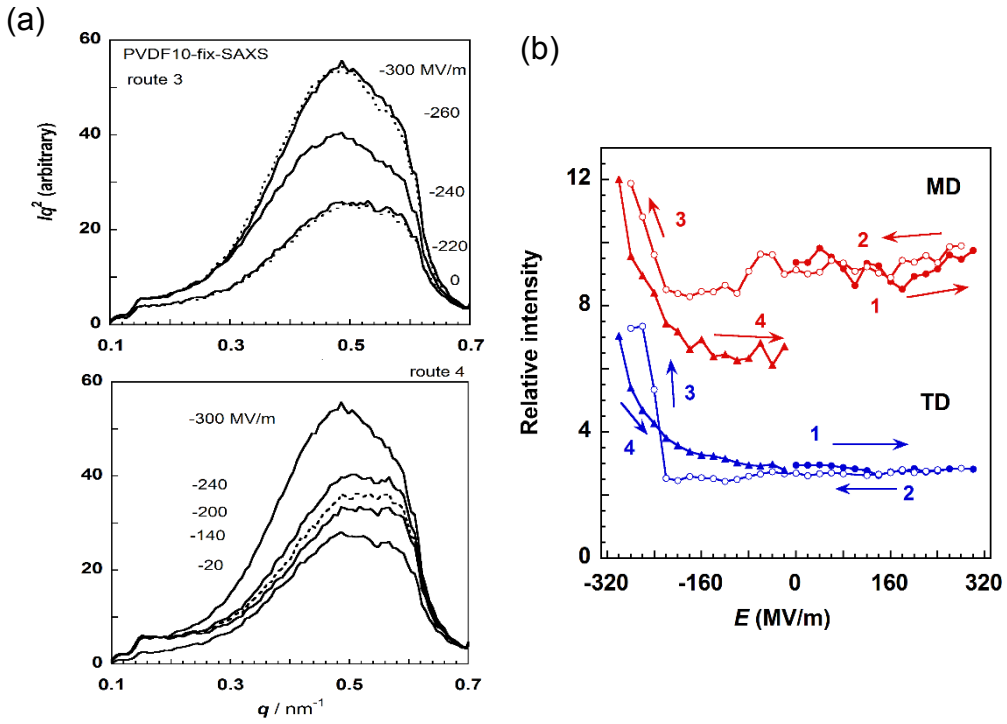

Figure S4-3 (a) The 1D SAXS profiles obtained from the peaks along the TD of the 2D data (Figure S4-1). (b) The electric field strength dependence of the integrated value of the Iq^2-q curves. The routes 3 and 4 in (a) correspond to those shown in (b). The intensity changed reversible in the high electric field strength region.

not clear at present to know an origin causing the change of Δρ and/or X_c. For example, by referring to such an observation that both of the SAXS intensities detected along the MD and TD increased at the same time, the applied electric field might increase the thermal fluctuation in the amorphous (or crystalline) region in the high E region to change the Δρ., resulting in the increment of the SAXS intensity. Or, the transformation from the α to β form in the high E region might be related to the change of Δρ and/or X_c. More detailed investigation is needed.

<FTIR> Figure S4-4 shows the IR spectra measured in parallel to the X-ray data collections. The spectral pattern of the initial sample is mainly that of the α form with the weak bands of the β form. By applying the voltage, many bands of the α and β forms were decreased in intensity. The reasons are (i) the α form changed to the δ form and (ii) the reorientation of CF_2 dipoles occurred by the electric field application. The 1209 cm^{-1} band of the α form disappeared on the way, the interpretation of which is made later. The integrated intensity of the 1275 cm^{-1} band, which corresponds to the CF_2 symmetric stretching mode of trans-zigzag chain, is plotted against the electric field strength as shown in Figure S4-5. In the first cycle, the intensity started to decrease sharply at around 80 MV/m. In the second process (from the maximal + 400 MV/m to - 400 M/m), the band did not change the intensity for a while and then it showed the peak at around -80 MV/m. In the third process going back toward the positive electric field direction, the intensity was low for a while, and then a peak was detected at around + 80 MV/m. After that, the change was repeated periodically (processes # 4 ~ #6) in the second circle. The similar hysteresis was detected also for the 610 cm^{-1} band of the α form (and δ) [CF_2 bending mode]. These observations are almost the same as reported in references 45 and 46 in the text. It should be noticed that the IR spectral data were successfully collected in both the first and second cycles different from the case of the X-ray measurement. The large IR beam covered the wider region of the electrode area than the quite small X-ray beam, and the IR signals from the parts outside the X-ray damaged area (but included in the electrode) were contained as the spectral components.

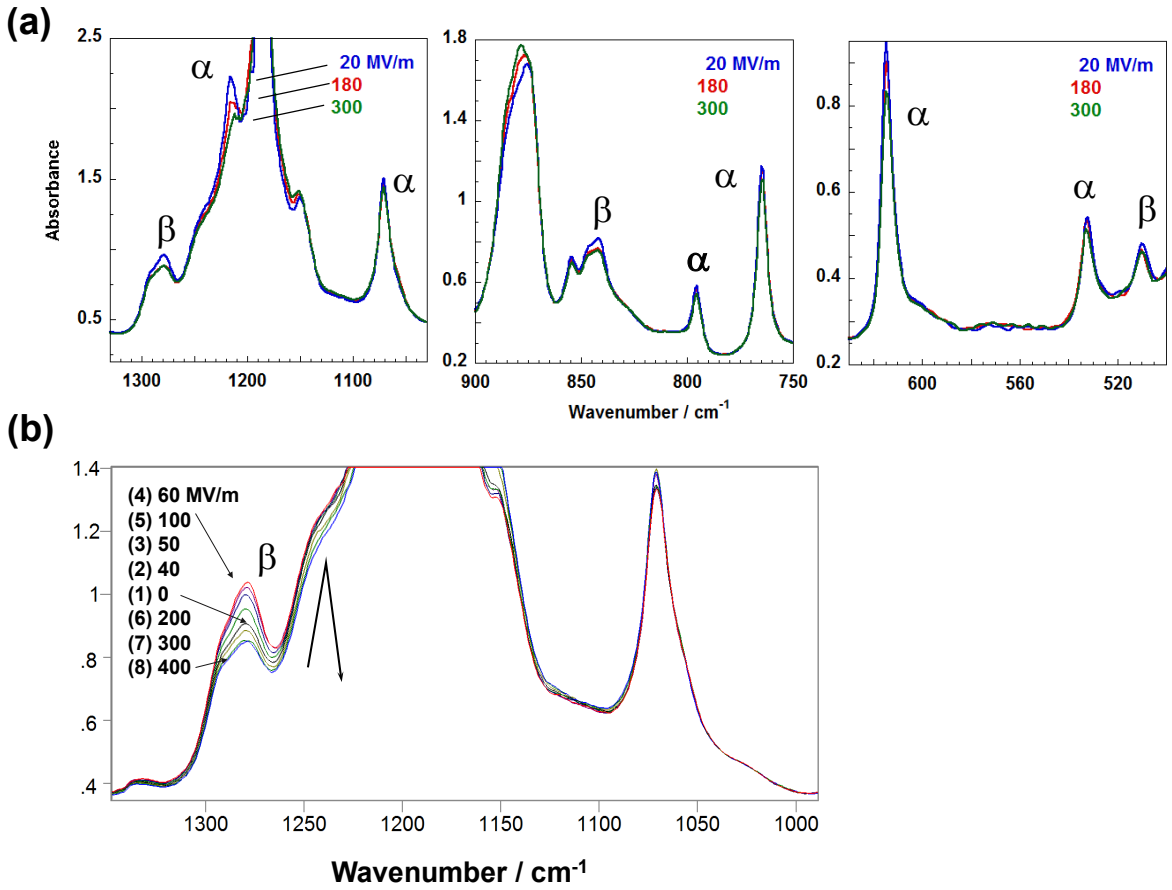

Figure S4-4. IR spectral changes of PVDF10 film measured simultaneously with the WAXD/SAXS data. The spectra in the several representative frequency regions are shown: (a) in the first cycle starting from the initial sample and (b) in the second cycle from 0 → 40 → 50 → 60 → 100 → 200 → 300 → 400 MV/m, as indicated by the numbers. In the first cycle (a), the bands of the α form, for example the 1209 cm^{-1} band, decreased the intensity by the application of electric field. In the second cycle (b), the 1275 cm^{-1} intrinsic to the trans-zigzag conformation decreased the intensity periodically as shown in Figure S4-5.

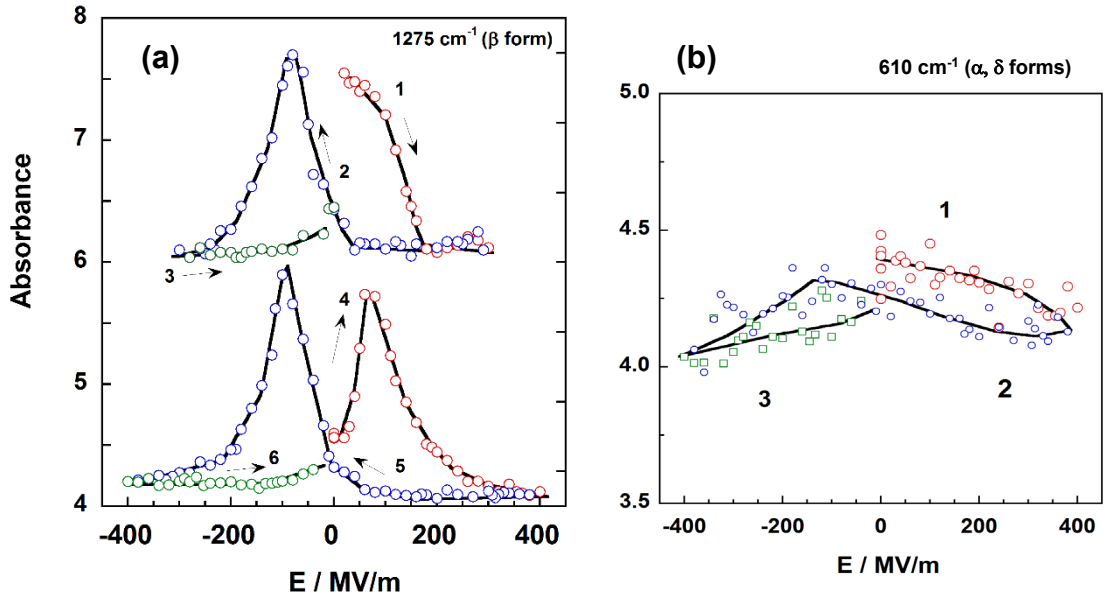

Figure S4-5. Electric field strength dependence of the integrated absorbance estimated for the IR bands of PVDF10 film subjected to a cyclic electric field (refer to Figure S4-4): (a) 1275 cm^{-1} band [the CF_2 stretching mode of trans-zigzag chain] and (b) 610 cm^{-1} band (the CF_2 bending mode of TGT$\bar{G}$ chain). The numbers indicate the order of the measurement route. The different colors are used for the plotted points to distinct the routes clearly. The intensities of the bands show the hysteresis loops in the periodical change of the electric field strength (trace the routes 1 – 2 – 3 – 4 – 5 – 6).

The summary of all of these experimental data is made in the text.

<IR spectrum of the δ form>

As seen in Figure S4-4, the IR bands of the α form changed by applying the electric field. These changes come from the α-to-δ transition by the poling treatment. For example, the 1182 cm^{-1} band remains even after the poling treatment, but the 1209 cm^{-1} band of the α form disappeared in the δ phase [see Figure S4-4 (a)]. They are assigned to the symmetric [$\nu_s(CF_2)$] and anti-symmetric CF_2

stretching [$\nu_{as}(CF_2)$] modes, respectively.[53,54] In the unit cell of the α form, these modes belong to the symmetry species A_u and the transition dipole is parallel to the *b* axis (μ' // *b*), as shown in Figure S4-6. In the δ-form cell, they may correspond, respectively, to the B_2 (// *b*) and A_2 (IR inactive) modes by assuming the factor group isomorphous to the point group C_{2v}. The 1182 cm^{-1} band of the B_2 species keeps the transition dipole along the *b* axis. But, for the 1209 cm^{-1} band, the two transition moments are canceled to give the null transition dipole (the A_2 species) and cannot be detected in the IR spectrum. The assignments of the other bands are referred to the literatures (7, 53, 54 in the text).

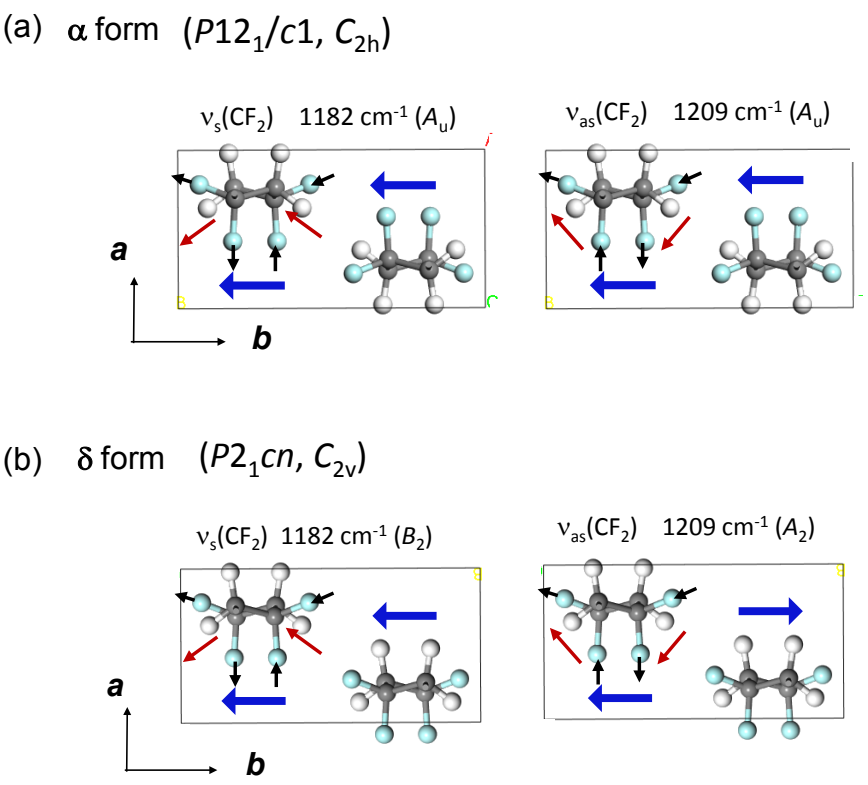

Figure S4-6. The symmetric and anti-symmetric CF_2 stretching modes in the unit cell of (a) the α form and (b) the δ form.

<Supporting Information 5> WAXD and SAXS data collected for PVDF30 film with the synchrotron X-ray beam irradiated on the fixed sample position

Figure S5-1 shows the electric field strength dependence of the 2D WAXD patterns measured for the PVDF30 film with the X-ray beam incident on the *fixed position* of the film. The behavior was essentially the same as that observed for the PVDF10 sample (see the supporting information 4). Figure S5-2 shows the 1D diffraction profiles obtained by the integration of the 2D patterns. In the first stage of increasing voltage, the 020(α) and 021(α) diffraction peaks of the α form became weaker and the 200/110(β), 001(β) and 111(β) peaks increased in intensity, indicating the partial transition from the α form to the β form. The 100(α) (shoulder, at $2\theta \sim 11^{o}$) and 120(α) (shoulder, at $2\theta \sim 17^{o}$) peaks of the α form, which were originally hard to see in the *through* pattern because of the preferential orientation of the *a* axis normal to the film surface, disappeared totally after the transition to the polar crystal form δ. In the second cycle from +250 MV/m to -250 MV/m, the diffraction intensity of the observed peaks decreased as a whole. By returning from -250MV/m in the third cycle, the 001(β), 111(β) and 021(α) peaks were observed to increase the intensity slightly but the intensity was quite weak.

Figure S5-3 shows the integrated intensity plotted against the electric field strength. The 021(α) peak decreased the intensity continuously in the repeated processes, originating from the damage by the strong X-ray beam. The intensity change of the 001(β) (and 111(β)) of the β form was quite noisy and could not be evaluated clearly for the quantitative analysis. As a trial, the intensity of the 001(β) peak was reduced by using the gradually-decreasing 021(α) peak intensity by assuming that the decrease of the latter peak intensity was due to the sample damage. However, the clear tendency could not be detected.

The similar intensity reduction in the course of the measurement was observed for the SAXS data as seen in Figures S5-4 and S5-5. The SAXS profile itself did not change very much in the

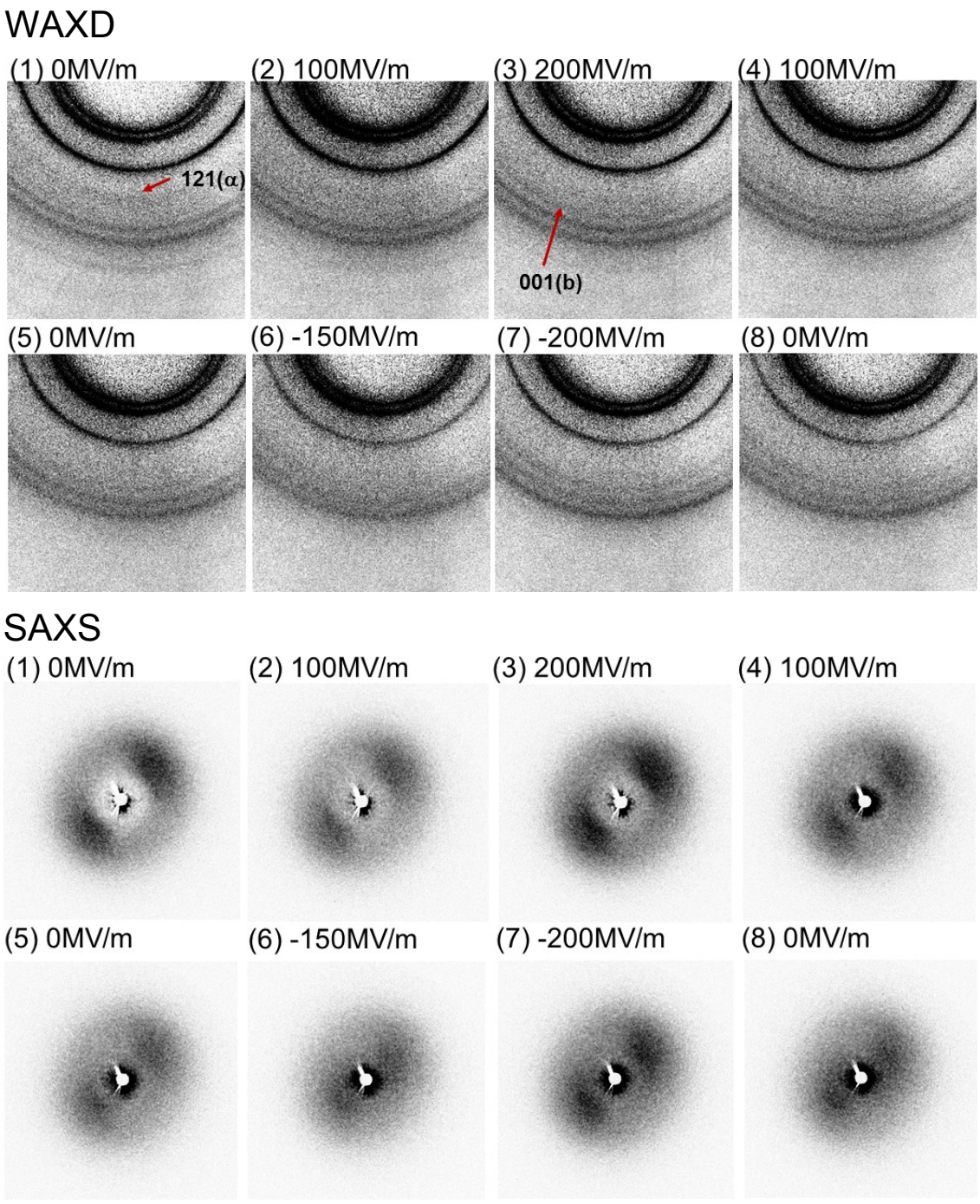

Figure S5-1. Series of the 2D-WAXD and SAXS patterns measured at the fixed position of the PVDF 30 film in the cyclic change of the electric field strength. The peaks of the original α form [121(α) *etc*.] disappeared after the transformation to the δ form, and the peaks of the β form [001(β)] increased the intensity. The SAXS pattern itself did not change mostly although the intensity changed in the process. It must be noted that the SAXS patterns are different from those given in the supplementary information 1: the -45^{o}-tilted pair of peaks are weak compared with the 4-points patterns with almost the same intensity in the latter case. This type of the pattern change occurs when the sample pieces are cut out at the different positions of the film sheet (center or off-center). The symmetric 4-points pattern might come from the sample piece cut along the central line of the film.

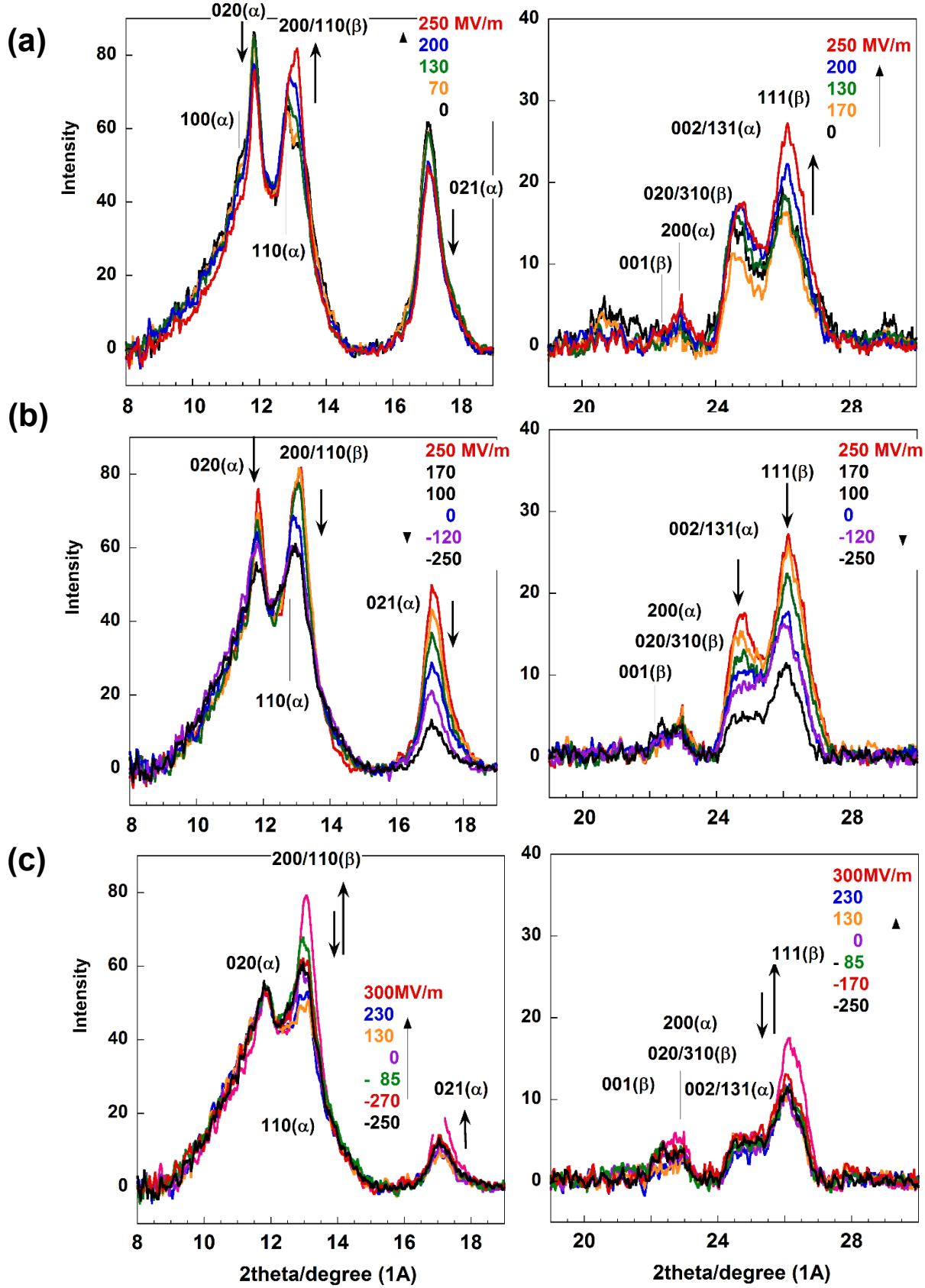

Figure S5-2. A series of the 1D WAXD profiles obtained from the 2D diffraction patterns of PVDF30 sample (Figure S5-1). The voltage was applied to the sample (a) from 0 to 350 MV/m, (b) from 350 to – 350 MV/m and (c) from – 350 to + 300 MV/m. The numeric symbol "020_2" indicates the 020 diffraction peak of the form II (or IIp).

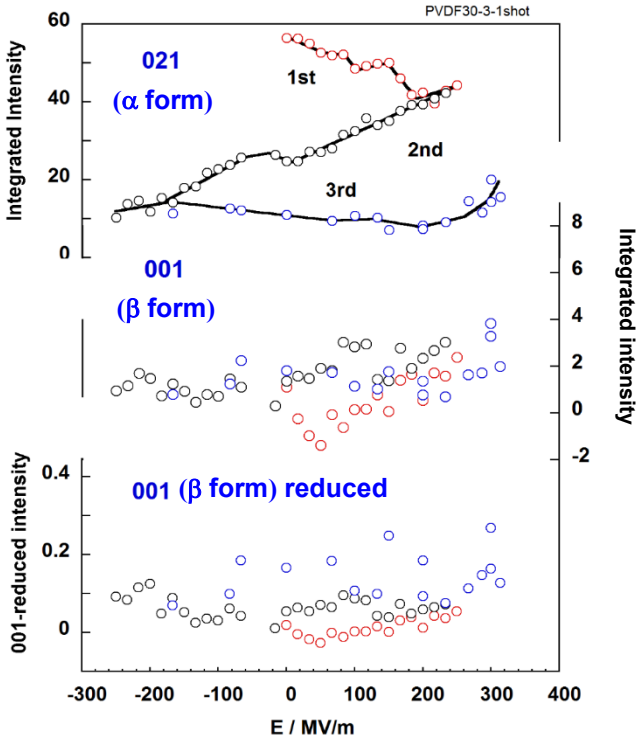

Figure S5-3. The electric-field-strength dependence of the integrated intensity of the 001(β) and 021(α) peaks evaluated for the WAXD data of the position-fixed PVDF30 sample. The intensity of the 021(α) peak decreased continuously in the cycles 1, 2 and 3. The 001(β) peak intensity was quite noisy, and no systematic tendency was extracted successfully. The plot of the 001(β) intensity reduced by the intensity of the 021(α) peak is shown also, but the systematic tendency cannot be extracted clearly.

application of electric field (Figure S5-4), suggesting the reservation of the higher-order structure of the stacked lamellae in the process. The integrated intensity plotted against the electric field strength increased or decreased depending on the electric field strength. In particular the intensity near the maximal electric field strength of about 300 MV/m became remarkably large, the phenomenon was similar to that observed for PVDF10 sample measured at one fixed point as shown in Figure S4-3 of the supporting information 4.

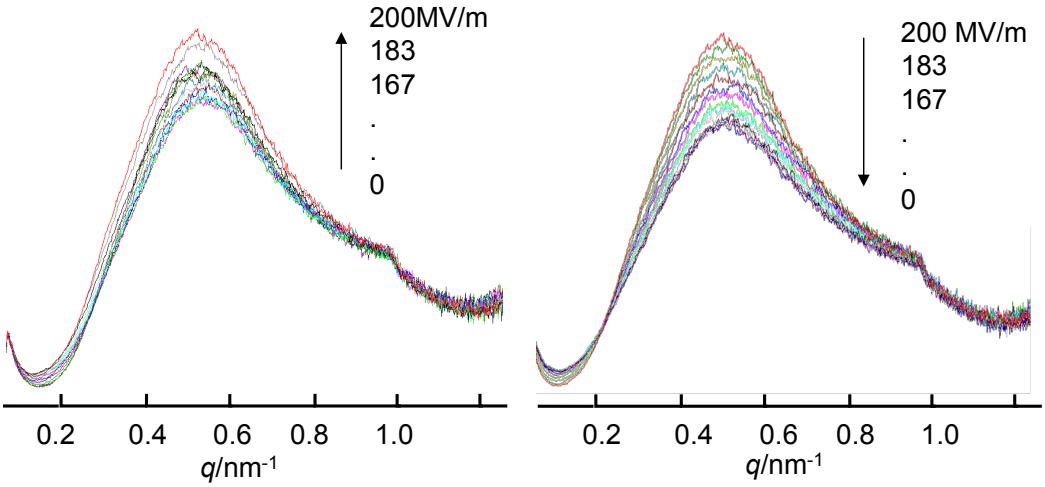

Figure S5-4 Electric field strength dependence of the 1D SAXS profiles (Iq^2-vs-q plot) obtained from the 2D SAXS patterns shown in Figure S4-1. The q is a scattering vector defined as $q = (40/\lambda)\sin(\theta)$ for the Bragg angle 2θ where λ = 1.0 Å.

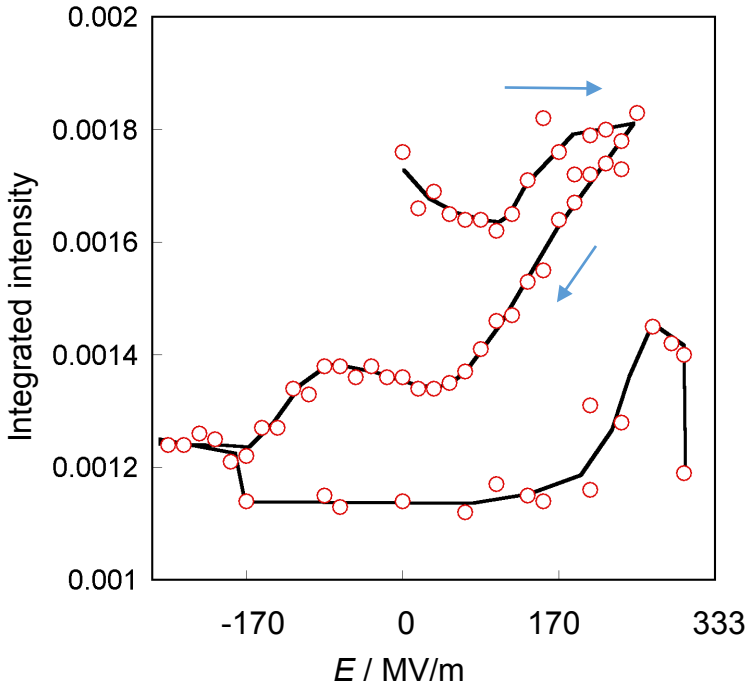

Figure S5-5 Electric field strength dependence of the integrated SAXS intensity based on the data given in Figure S5-4. The absolute value itself decreased gradually with the process, although the temporary increase and decrease of the intensity are detected. In the electric field strength region near 300 MV/m, the SAXS intensity became appreciably high. This is similar to that observed for PVDF10 sample (the supporting information 4)